Boundary-Layer Receptivity

Anthony J. Dietz

Accurate prediction of boundary-layer transition is crucial to the solution of a wide range of fluid dynamics problems, from the design of low-drag airfoils to the estimation of reentry heat loads. In many flows, transition begins with a receptivity process, in which boundary-layer instabilities are excited by disturbances in the free stream. Understanding of this process has come a long way in recent years. A particular Ames contribution has been in the area of receptivity to vortical disturbances.

An experiment was conducted in a low-turbulence research wind tunnel to investigate the vortical receptivity mechanism in a controlled flow. Small vortical disturbances were introduced into the free stream by a vibrating ribbon, and the effect of these disturbances on the boundary layer of a flat plate was measured with hot-wire anemometry. According to current receptivity theory, a receptivity site with a short-scale variation in the boundary-layer mean flow is required to convert the typically long-wavelength free-stream disturbances into short-wavelength boundary-layer instabilities. Strips of very thin polyester tape were fixed to the surface of the plate to provide such a site.

The first series of tests involved continuous single-frequency disturbances. No instability waves could be detected without roughness on the plate. However, with roughness present, instability waves were measured at downstream locations. The mode shape, growth rate, and phase speed of the waves matched that of the Tollmien-Schlicting (TS) waves predicted by linear-stability theory. Linear-stability calculations were then used to determine the immeasurably small initial amplitudes of the waves at the roughness location from amplitudes measured downstream, thus separating the receptivity (generation) characteristics of the waves from their stability (growth) characteristics.

The experimentally obtained receptivity coefficients agreed well with those predicted by receptivity theory, and both followed similar trends with frequency and Reynolds number. However, these results pertained to continuous single-frequency waves, whereas real-world flows contain broadband transient disturbances. Broadband pulse and random disturbances could also be generated by the ribbon. The response to a pulse disturbance is shown in the first figure, where a TS wave packet, generated by an interaction between the convected pulse and the surface roughness, can be seen lagging the pulse disturbance. The lower propagation speed of the wave packet has separated the two phenomena, allowing each to be analyzed independently.

The receptivity coefficients calculated for pulse and random disturbances are compared with single-frequency coefficients in the second figure. Similar results were obtained for all three disturbance types, demonstrating that the single-frequency theories are applicable to transient and broadband disturbances. The results also confirmed theoretical predictions that receptivity to distributed roughness is nearly an order of magnitude greater than that for single roughness, and that the results for distributed roughness are highly tuned to a resonant frequency at which waves generated at successive roughness elements are in phase and add constructively.

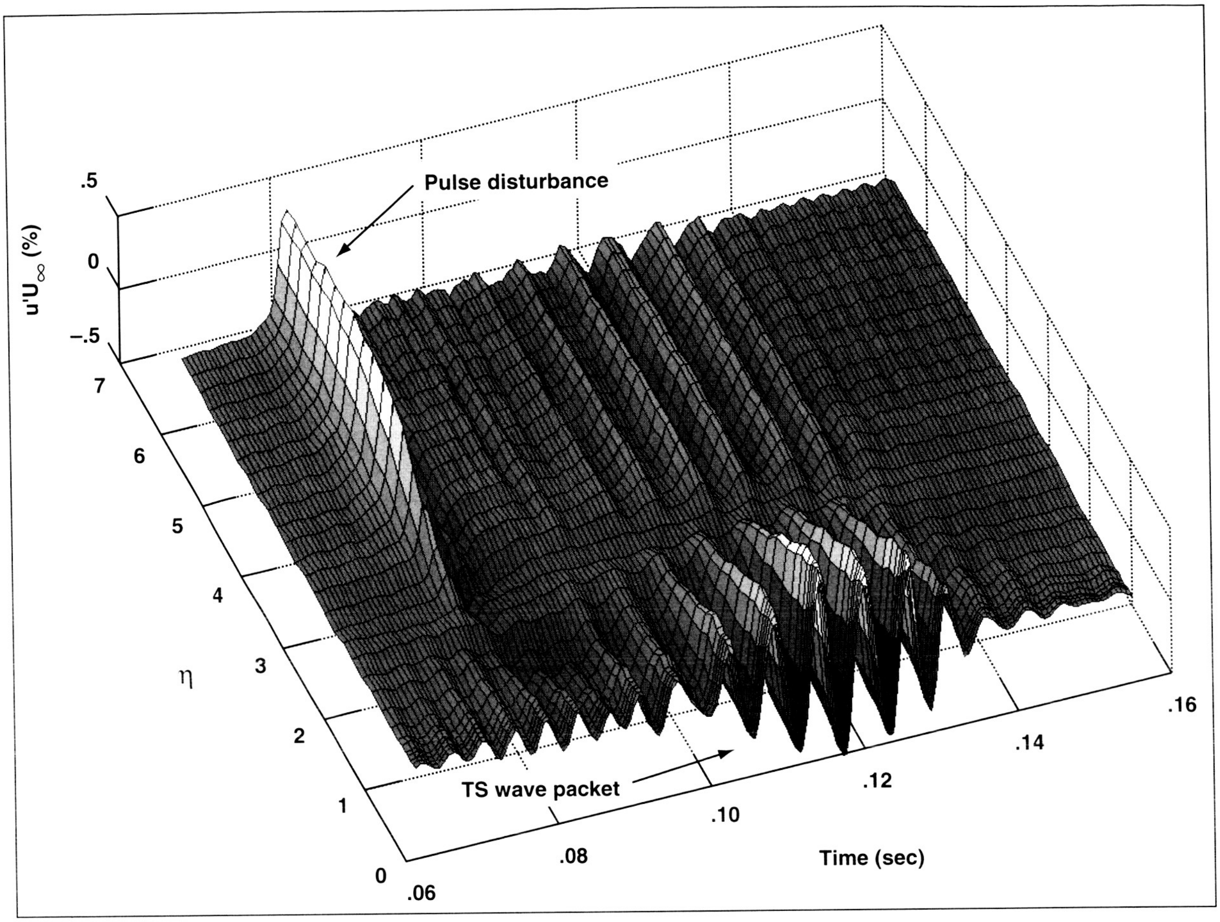

Fig. 1. Boundary-layer response to a pulse disturbance measured downstream of an array of roughness elements. Phase-locked averaged time records of the streamwise velocity fluctuations u', normalized by the free-stream velocity U_∞, are plotted against the nondimensional height above the plate surface $\eta = y/(2\nu x/U_\infty)^{1/2}$.

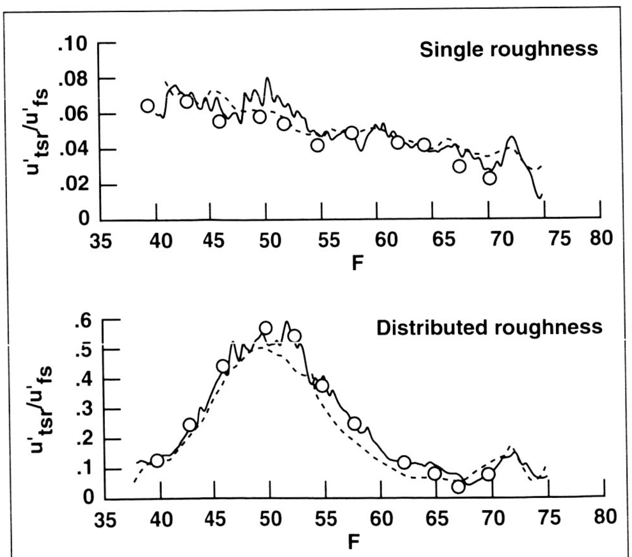

Fig. 2. Variation of receptivity coefficient with frequency for three disturbance types at single and distributed roughnesses. TS wave amplitude at the roughness location (u'tsr) normalized by the free-stream disturbance amplitude at the edge of the boundary layer (u'fs) plotted against the frequency parameter $F = 2\pi f \nu/U_\infty^2 \times 10^6$; single frequency (o), pulse (- - -), random (——).

This experimental verification of the mechanism behind receptivity to convected disturbances is a step toward the still-unrealized goal of transition criteria, which include free-stream disturbance characteristics. Current prediction techniques do not take the free-stream disturbance environment into account and so miss an important aspect of the problem.

Point of Contact: A. Dietz
(650) 604-4137
adietz@mail.arc.nasa.gov

Evolution of Strained Plane Wakes

Michael M. Rogers

Turbulence models currently have difficulty predicting the response of turbulence to additional strains, such as those arising in the flow over a multicomponent airfoil designed to produce high lift. In particular, as the turbulent wake of an upstream airfoil component encounters the pressure gradient produced by a downstream component, it is strained. The response to this strain is poorly predicted by existing turbulence models.

In order to provide insight into the behavior of such flows and to provide a database to aid turbulence modelers, several direct numerical simulations of strained plane wakes have been generated. These simulations are made in a reference frame moving with the free-stream velocity outside the wake and thus they evolve in time. Such temporally evolving flows are computationally simpler to generate and therefore it is possible to achieve higher Reynolds numbers and more realistic turbulence. In the limit of small wake deficits the equations governing the temporally evolving problem are identical to those describing a spatially evolving flow, such as that of a wake in an adverse pressure gradient.

Previous direct numerical simulations of unstrained wakes have been used to generate the initial conditions for the strained wake computations. Once the unstrained wake reaches an apparently self-similar state, the strain is applied to generate the strained wake cases. Six different plane strain geometries have been applied to the wake, with the directions of compression and expansion associated with the strain being aligned with the coordinate axes. The case with compression in the streamwise direction and expansion in the cross-stream (inhomogeneous) direction corresponds to that of a wake developing in the presence of an adverse pressure gradient.

Analysis shows that there is a possible self-similar state for wakes subjected to strain applied at a constant rate. Both the peak velocity deficit of the wake and the wake width are predicted to evolve exponentially in time, with the exponent in both cases being equal to half of the difference between the cross-stream and streamwise total strains. All the Reynolds stresses are predicted to scale with the square of the peak velocity deficit in this self-similar state.

The simulated flows typically do not evolve according to this self-similar solution, although the wake velocity deficits and widths do change exponentially. The wake width in flows that are compressed in the cross-stream direction approaches a constant, whereas it increases exponentially at the same rate as the global strain in flows that are expanded in the cross-stream direction (see figure). For flows in which the cross-stream direction is unstrained the wake spreads at a rate that is similar to the unstrained case. For the case that is analogous to a wake developing in an adverse pressure gradient this is consistent with the rate predicted by the self-similar analysis, and indeed this case does appear to be evolving in accord with the predicted self-similar solution.

The wake mean velocity profile is largely unaffected by the geometry of the strain, remaining approximately Gaussian throughout the flow evolution in all cases. The behavior of the Reynolds stresses, however, varies dramatically, depending on the strain geometry and on whether the global mean strain produces or destroys a particular Reynolds stress component. In most cases (although not in the adverse pressure gradient case), the mean shear